# Correlated Geometric Scaling of Tornado Damage Paths in the SPC Database (1950–2024)

Waleed Mouhali[1]

[1]Applied Mathematics Department, LYRIDS Laboratory, ECE Paris, 10 rue Sextius Michel, 75015 Paris, France

**Correspondence:** Waleed Mouhali (waleed.mouhali@ece.fr)

**Abstract.**

Despite the remarkable variability of individual tornadoes, it remains unclear whether their damage-path geometry exhibits statistically robust large-scale organization. Using a catalogue of 69,975 tornadoes from the U.S. Storm Prediction Center spanning the period 1950–2024, we investigate the statistical relationship between reported tornado path length and maximum path width over more than seven decades of observations.

We find that the average path width increases systematically with path length according to an effective empirical scaling relationship characterized by a stable exponent of approximately 0.43. This relationship remains remarkably consistent across successive historical periods and is robust to intensity-based sensitivity analyses. Building on this result, we examine a geometry-based area proxy and show that its statistical behaviour follows directly from the observed width–length relationship. Higher-order moment analyses reveal a predominantly affine scaling spectrum over the resolved range, while null-model experiments demonstrate that neither heavy-tailed marginal distributions nor random combinations of independent variables reproduce the observed geometric organization.

The measured exponent should not be interpreted as a deterministic law governing individual tornadoes, but rather as an effective population-level descriptor of the average geometry of tornado damage paths. These results indicate that, despite substantial event-to-event variability, a robust statistical organization emerges across nearly 70,000 observations. The present framework provides a quantitative benchmark for future dynamical and environmental investigations of tornado-path geometry and its possible physical origins.

## 1 Introduction

Tornadoes are among the most extreme and intermittent manifestations of atmospheric convection, arising from strongly nonlinear interactions involving moist instability, vertical wind shear, mesocyclonic rotation, vortex stretching, boundary-layer turbulence, and dissipative processes acting across a broad range of spatial and temporal scales. Although major advances have been achieved in severe-weather forecasting, Doppler-radar observations, and post-event damage surveys, the collective statistical organization of tornado damage paths remains only partially understood. Tornado climatology has extensively characterized occurrence frequencies, seasonal variability, geographical distributions, and intensity statistics, yet much less is known about whether robust geometric relationships emerge from the highly heterogeneous population of observed tornadoes.

Most classical tornado studies have focused primarily on descriptive statistics associated with the Fujita and Enhanced Fujita classifications. Brooks (2004) showed that tornado path length and path width both increase systematically with tornado intensity and exhibit broad non-Gaussian distributions spanning several orders of magnitude. Subsequent studies further demonstrated that tornado-path geometry contains physically meaningful information beyond discrete intensity classifications. In particular, Elsner et al. (2014) proposed continuous intensity estimators based on tornado dimensions, suggesting that damage-path geometry reflects underlying properties of vortex organization and parent-storm dynamics.

The interpretation of long-term tornado statistics, however, is complicated by substantial observational inhomogeneities. Agee and Childs (2014) emphasized that historical tornado databases are affected by evolving reporting practices, increasing population density, improvements in damage surveys, and changes in tornado classification methodologies. Likewise, Edwards et al. (2021) showed that the deployment of Doppler-radar networks and the transition from the original Fujita scale to the Enhanced Fujita scale significantly modified tornado detection capabilities, particularly for weak tornadoes. Consequently, any statistical relationship identified from long-term tornado records must be interpreted in the context of these observational limitations and tested for robustness across different historical periods.

Beyond descriptive climatology, several studies have suggested that severe convective systems exhibit statistical properties analogous to those encountered in complex nonlinear systems. Malamud and Turcotte (2012) analysed tornado outbreaks using concepts inspired by statistical physics and self-organized criticality, reporting approximate scale-free behaviour in outbreak statistics and tornado-path distributions. Tippett and Cohen (2016) further demonstrated that tornado outbreak variability approximately follows Taylor scaling laws, where the variance increases as a power of the mean outbreak rate. Such behaviour is characteristic of multiplicative amplification processes and suggests the emergence of multiscale statistical organization within severe convective activity.

More generally, atmospheric science has progressively incorporated concepts originating from turbulence theory, multiplicative cascades, and multifractal analysis. Since the pioneering work of Lovejoy and Schertzer (1985), numerous studies have shown that precipitation, cloud fields, hydrological extremes, atmospheric radiative fields, and geophysical turbulence exhibit hierarchical scaling behaviour and heavy-tailed statistics over broad ranges of scales (Schertzer and Lovejoy, 1987; Tessier et al., 1993; Veneziano et al., 2006; Lovejoy and Schertzer, 2013). Similar forms of statistical organization have also been identified in other nonlinear geophysical systems. Earthquake occurrence obeys the Gutenberg–Richter law and exhibits scale-free clustering properties (Turcotte, 1997; Corral, 2004); wildfire areas display heavy-tailed size distributions and finite-size scaling behaviour (Malamud et al., 1998); avalanches, fragmentation processes, and river-network statistics likewise reveal emergent organization characteristic of strongly nonlinear nonequilibrium systems (Bak et al., 1987; Stanley et al., 1999; Sornette, 2006). Collectively, these studies suggest that robust statistical organization may emerge from complex geophysical systems despite strong local stochasticity.

Recent work has also emphasized that the energetics of atmospheric motion should be interpreted within the broader framework of atmospheric thermodynamics rather than solely in terms of wind kinetic energy, providing additional perspective on the interpretation of large-scale atmospheric scaling relationships (Tuck, 2025).

Despite this extensive literature on atmospheric scaling and geophysical intermittency, tornado damage paths themselves have rarely been investigated from the perspective of correlated geometric organization. Most previous studies have considered tornado path length, path width, intensity distributions, or outbreak frequencies as largely independent climatological observables. Although broad heavy-tailed behaviour has occasionally been reported, the existence of statistically robust relationships linking tornado path length and path width across a large heterogeneous population remains largely unexplored.

A further challenge concerns the interpretation of energetic observables. Direct kinetic-energy measurements are unavailable at climatological scales, and long-term tornado databases primarily contain geometrical descriptors together with discrete EF intensity classes. Consequently, energy-related quantities necessarily rely on proxies combining path geometry and intensity weighting, potentially introducing circularity into scaling analyses. Recent work has also emphasized that reconstructing tornado wind fields from damage observations remains a challenging inverse problem and that atmospheric wind kinetic energy represents only a small fraction of the total atmospheric energy budget (Miller et al., 2024; Tuck, 2025). For this reason, the present study first investigates the geometry of tornado damage paths themselves before considering any derived geometry–intensity observable.

Using the NOAA Storm Prediction Center (SPC) tornado database covering the period 1950–2024, we examine the statistical relationship between reported tornado path length and reported maximum path width. The analysis combines heavy-tail statistics, finite-size scaling, local scaling diagnostics, conditional moment analysis, and null-model comparisons inspired by statistical physics and nonlinear dynamics. Particular attention is devoted to determining whether the observed statistical organization reflects genuine correlations between path length and path width or merely the trivial consequences of broad marginal distributions, observational inhomogeneities, or derived geometric quantities.

Rather than seeking a deterministic law governing individual tornadoes, our objective is to determine whether robust statistical organization emerges at the population level despite the remarkable variability of individual events. We therefore assess the robustness of the observed geometric relationship across independent historical periods, tornado-intensity subsets, and complementary statistical diagnostics. Finally, we discuss the extent to which the observed organization may be interpreted as an effective population-level property and place it within the broader context of nonlinear geophysical systems, atmospheric scaling, and intermittency theory.

## 2 Methods

### 2.1 Tornado database and observational framework

The present study uses the NOAA Storm Prediction Center (SPC) tornado database covering the period 1950–2024. The catalogue provides, for each confirmed tornado event, the date and location of occurrence, geographical coordinates, reported path length, reported maximum path width, and Fujita or Enhanced Fujita intensity classification. The original Fujita and the Enhanced Fujita scales are here treated jointly through the corresponding EF0–EF5 categories.

Only events with strictly positive reported path length and maximum path width were retained. After removal of missing or non-physical values, the final sample contains 69 975 tornadoes. Path lengths, originally reported in miles, were converted to kilometres, while path widths, originally reported in yards, were converted to metres.

The SPC archive is an event-level catalogue rather than a gridded observational product. Consequently, the data do not possess a single uniform spatial resolution. Each record contains reported geographical coordinates and damage-path attributes obtained from storm reports and post-event surveys, whose precision varies across events and observational periods.

Throughout this study, $L$ denotes the reported tornado path length and $W$ the reported maximum path width. The latter is an observational damage-survey quantity and should not be interpreted as the instantaneous physical diameter of the tornadic vortex. Near-surface wind speed decreases continuously with radial distance from the vortex core, and winds outside the documented damage path may remain elevated above the background flow without exceeding locally effective damage thresholds. The reported value of $W$ therefore depends not only on tornado dynamics, but also on the availability of damage indicators, land use, surface roughness, structural vulnerability, and post-event survey practices.

The interpretation of long-term tornado statistics is further complicated by substantial changes in observational capability. Historical records are affected by evolving reporting practices, increasing population density, improvements in damage assessment, and changes in tornado-classification procedures (Agee and Childs, 2014; Edwards et al., 2021). In particular, weak and short-lived events were more likely to remain undetected during the early part of the record, whereas the progressive deployment of Doppler radar and the standardisation of storm surveys increased detection and reporting completeness during recent decades.

Rather than attempting to reconstruct event-specific observational uncertainties over the full 75-year record, we assess the robustness of the statistical results by repeating the analysis over three independent historical periods: 1950–1974, 1975–1999, and 2000–2024. These subsets contain 15 934, 24 216, and 29 825 tornadoes, respectively. They approximately represent an early observational period, a transitional period, and the modern Doppler-radar era. Agreement between these subsets is interpreted as evidence of population-level robustness, but not as proof that the underlying path-width measurements are free of historical bias.

## 2.2 Geometric and intensity-weighted observables

The primary objective of this study is to determine whether tornado damage paths exhibit statistically robust geometric organization independently of any energetic weighting procedure. We therefore begin by analysing the two fundamental quantities directly reported in the SPC catalogue: the tornado path length, denoted by $L$, and the reported maximum path width, denoted by $W$.

The principal relationship investigated throughout this work is the empirical scaling relation

$$W \propto L^{\alpha}, \tag{1}$$

where $\alpha$ denotes an effective scaling exponent estimated from the complete tornado population. Throughout this study, $\alpha$ is not interpreted as a universal dynamical constant governing the evolution of individual tornadoes. Rather, it provides a statistical descriptor of the average geometric organization emerging from a large and heterogeneous population of observed tornadoes.

From these two directly observed quantities, we define the geometry-only observable

$$A = LW, \tag{2}$$

which represents a simple geometrical proxy describing the overall extent of the reported damage path. The quantity $A$ should not be interpreted as the exact physical damage area, since the actual affected surface depends on numerous factors including land use, structural vulnerability, damage continuity, and local survey practices. Instead, $A$ is employed as a coarse-grained geometrical descriptor allowing us to examine whether the statistical organization identified through Eq. (1) remains consistent across several complementary analyses.

Although the principal focus of the present work concerns geometric organization, we also consider an intensity-weighted observable in order to compare purely geometric statistics with a simple geometry–intensity proxy. Following previous studies relating tornado intensity to damage characteristics (Brooks, 2004; Elsner et al., 2014), each EF category is associated with a representative wind-speed amplitude derived from the operational NOAA wind-speed intervals. We then define

$$E \propto V^2 LW, \tag{3}$$

where $V$ denotes the characteristic wind speed assigned to the corresponding EF category.

The observable $E$ is not intended as an estimate of the true kinetic energy of a tornado. Atmospheric kinetic energy represents only a small fraction of the total atmospheric energy budget, which is dominated by internal and gravitational potential energy (Gill, 1982; Dutton, 1986). Moreover, the SPC database does not contain direct measurements of vortex velocity, but only discrete EF intensity classes. Consequently, Eq. (3) should be regarded as a phenomenological geometry–intensity proxy rather than a dynamical energy measure.

Because the assigned wind speeds take only a finite number of discrete values, the observable $E$ inevitably inherits part of the discretization associated with the EF classification. For this reason, the principal conclusions of the present study are based on the geometry-only observables $L$, $W$, and $A$, whereas the analysis of $E$ is used primarily as a secondary robustness test to determine whether the observed geometric organization remains qualitatively unchanged after coarse intensity weighting.

### 2.3 Statistical analysis

The effective scaling relationships were estimated in logarithmic coordinates using ordinary least-squares (OLS) regression. For two positive observables $X$ and $Y$, we assume the empirical relation

$$Y \propto X^{\eta}, \tag{4}$$

which becomes

$$\log_{10} Y = \eta \log_{10} X + c, \tag{5}$$

where $c$ denotes the intercept and $\eta$ the effective scaling exponent.

The principal regressions considered in this study concern the relationships between tornado path width and path length (Eq. 1), the geometry-only observable (Eq. 2), and the energy-weighted observable (Eq. 3). The coefficient of determination ($R^2$) is reported for each regression as a measure of the fraction of variance explained in logarithmic space.

Because tornado geometry exhibits substantial intrinsic variability, the event-level OLS regression alone does not fully characterize the underlying statistical organization. We therefore complement the global fit by computing conditional median path widths within logarithmically spaced path-length bins. These conditional statistics provide a robust estimate of the central tendency of the width–length relationship while reducing the influence of local sampling fluctuations and extreme events.

Uncertainties associated with both the event-level regressions and the conditional statistics were estimated by bootstrap resampling. Event-level confidence intervals were obtained using pairs-bootstrap realizations, whereas conditional medians were resampled independently within each logarithmic length bin. Unless otherwise stated, the reported confidence intervals correspond to the 2.5th and 97.5th percentiles of the bootstrap distributions.

To evaluate whether the measured exponents remain stable across the historical tornado record, all analyses were repeated independently for the three observational periods introduced in Section 2.1. Additional sensitivity analyses were performed using progressively restricted tornado populations (EF1+, EF2+, and EF3+) in order to assess the influence of tornado intensity on the estimated scaling exponents.

The dispersion surrounding the population-level trend was also examined as a function of path length. The progressive broadening visible in the event-density field and conditional statistics is interpreted as heteroscedasticity associated with the heterogeneous tornado population, rather than as scale-independent observational noise. Accordingly, the fitted exponent is used to characterize the evolution of the central tendency and not to predict individual tornado widths.

Throughout this study, the estimated exponents are interpreted as effective statistical descriptors of the average geometric organization of the tornado population rather than as deterministic laws governing individual tornadoes. In particular, the presence of broad dispersion, heteroscedasticity, observational uncertainty, and population heterogeneity implies that the measured exponents should not be regarded as asymptotic critical exponents in the sense of statistical physics, but rather as empirical descriptors of the dominant large-scale statistical organization present in the SPC catalogue.

### 2.4 Distribution and scaling diagnostics

The statistical organization of tornado geometry was investigated using a set of complementary diagnostics designed to characterize both the marginal distributions of the observables and the robustness of the measured scaling relationships. Throughout this section, no single diagnostic is interpreted in isolation; rather, consistency among several independent statistical measures is taken as evidence for robust population-level organization.

We first examine the marginal distributions of the geometric observables using complementary cumulative distribution functions (CCDFs). Compared with probability density functions, CCDFs are less sensitive to binning choices and provide a more stable representation of the distribution tails. They therefore allow a direct comparison between historical periods over the full observable range while preserving the behaviour of rare extreme events.

To evaluate whether the distributions exhibit scale robustness across the different observational periods, we perform finite-size scaling (FSS) analysis. Following standard approaches used in statistical physics, each distribution is rescaled by an appropriate characteristic scale before being compared across the three historical subsets. Successful collapse of the rescaled distributions is interpreted as evidence of statistical robustness across observational periods, rather than as proof of strict universality in the underlying tornado dynamics.

Beyond the marginal distributions, we investigate the scaling behaviour of conditional moments. For an observable $X$ conditioned on tornado path length $L$, the moments are defined as

$$M_q(L) = \langle X^q \,|\, L \rangle\,, \tag{6}$$

where $q$ denotes the moment order.

The principal analysis focuses on the interval

$$0.25 \leq q \leq 2,$$

for which the estimates remain statistically well constrained over the full catalogue. Higher-order moments,

$$2 < q \leq 3,$$

are examined only as exploratory sensitivity analyses because they become increasingly dominated by the rarest extreme events and therefore exhibit larger statistical uncertainty.

For each moment order, effective scaling exponents are estimated from the dependence of $M_q(L)$ on path length. The resulting scaling spectrum is then examined in order to determine whether the hierarchy is compatible with a predominantly affine organization or exhibits statistically significant departures from linearity. Particular attention is paid to the bootstrap uncertainty associated with the estimated spectrum so that weak apparent curvature is not overinterpreted as evidence of multifractality.

Finally, local scaling exponents are computed by evaluating successive finite differences of the logarithmic conditional statistics between adjacent logarithmic path-length bins. Unlike global regressions, these local estimates make it possible to identify possible scale-dependent departures from the average behaviour and to distinguish genuine changes in scaling from finite-sample fluctuations occurring at the smallest and largest path lengths.

Taken together, CCDFs, finite-size scaling, conditional moments, and local scaling diagnostics provide complementary information on the robustness of the observed geometric organization. Agreement among these independent diagnostics strengthens the interpretation of the measured exponents as effective statistical descriptors of the tornado population rather than artefacts arising from a particular estimation procedure.

### 2.5 Local scaling exponent

Finally, we investigate the local scaling exponent defined by

$$\eta(L) = \frac{d \log A}{d \log L}.$$

Conditional median values of the geometry-only observable were first computed within 24 logarithmically spaced path-length bins. Bins containing fewer than 80 tornadoes were excluded from the analysis, leaving 21 well-sampled bins. The local exponent was then estimated by successive finite differences between adjacent retained bins,

$$\eta_{\text{loc}} = \frac{\log A_{i+1} - \log A_i}{\log L_{i+1} - \log L_i},$$

and assigned to the corresponding intermediate logarithmic scale. The same logarithmic binning and minimum-sample criterion were applied throughout the analysis.

Figure 11 presents the evolution of this local exponent as a function of scale.

### 2.6 Null-model analysis

To determine whether the observed geometric organization arises from genuine correlations between tornado path length and path width, rather than from the broad marginal distributions of the individual variables, we compare the SPC observations with a series of progressively more restrictive null models.

The objective of these reference models is not to reproduce tornado physics, but to isolate the respective contributions of marginal distributions, finite sample size, and variable correlations to the observed statistical behaviour. A null model is therefore considered successful only if it reproduces the same ensemble of statistical diagnostics obtained from the observations, including the width–length relationship, the conditional moment hierarchy, and the finite-size scaling behaviour.

The first null model consists of independent random permutations of the observed path lengths and path widths. This procedure preserves the empirical marginal distributions of both variables while completely destroying their mutual correlation. Any statistical organization remaining after permutation therefore originates solely from the marginal distributions.

A second reference model is constructed from independent synthetic lognormal distributions adjusted to reproduce approximately the observed first- and second-order moments of the individual variables. The lognormal distribution is employed here only as a convenient broad-distribution reference model and is not intended to represent the full class of heavy-tailed atmospheric statistics. Its role is simply to evaluate whether broad positive distributions alone can generate the observed geometric organization.

Additional synthetic populations are generated by combining independent random realizations of path length, path width, and EF-class assignments. These experiments allow us to evaluate separately the influence of geometric correlations and coarse intensity weighting on the derived observables.

All null models are analysed using exactly the same statistical procedures as the SPC catalogue, including event-level regressions, conditional statistics, finite-size scaling, moment analysis, and local scaling diagnostics. This identical analysis pipeline ensures that any difference between observations and null models reflects the statistical structure of the data themselves rather than methodological differences.

Agreement or disagreement between the null models and the observations is therefore interpreted collectively across the complete set of diagnostics. No single statistical indicator is regarded as sufficient by itself to establish or reject the existence of correlated geometric organization. The null-model framework should therefore be viewed as a statistical falsification procedure rather than as an attempt to construct simplified models of tornado dynamics.

### 2.7 Reproducibility and computational implementation

All statistical analyses were performed using a common Python-based analysis pipeline developed specifically for this study. The same computational workflow was applied consistently to the complete SPC catalogue, to each historical subset, to the EF-restricted populations, and to all synthetic null models. Consequently, every statistical diagnostic presented in this work—including event-level regressions, conditional statistics, bootstrap confidence intervals, complementary cumulative distribution functions, finite-size scaling, conditional moment analysis, and local scaling diagnostics—was obtained using an identical processing chain.

Bootstrap confidence intervals were estimated from 2,000 resampling realizations. Event-level scaling exponents were obtained using pairs-bootstrap resampling, whereas conditional statistics were bootstrapped independently within each logarithmic path-length bin. Unless otherwise stated, all reported confidence intervals correspond to the 2.5th and 97.5th percentiles of the bootstrap distributions.

To facilitate direct comparison between observational periods and null models, identical logarithmic binning, fitting procedures, and graphical representations were employed throughout the study. This uniform analysis framework minimizes methodological differences between experiments and ensures that any observed variations originate from the statistical properties of the datasets themselves rather than from changes in the analysis procedure.

The computational workflow was designed to be fully reproducible from the publicly available NOAA Storm Prediction Center tornado database. All derived quantities were obtained using fixed and consistently applied analysis settings, without manual adjustment or case-specific parameter tuning. Random resampling procedures used fixed numerical settings and were applied identically across observational subsets and null models.

The objective of the present methodology is not to predict the geometry of individual tornadoes but to identify robust statistical organization at the population level. The agreement of independent diagnostics across multiple observational periods and sensitivity analyses is therefore interpreted as evidence of statistical robustness rather than proof of a universal dynamical law governing tornado evolution.

## 3 Results

### 3.1 Emergence of a population-level width–length relationship

We first investigate whether tornado damage-path geometry exhibits a systematic statistical organization independently of any intensity weighting. Figure 1 presents the relationship between reported tornado path length $L$ and reported maximum path width $W$ for the complete SPC catalogue using a logarithmic hexagonal density representation together with the global event-level regression and the conditional median widths computed within logarithmically spaced path-length bins.

Several features emerge directly from the observations. First, reported maximum path width increases systematically with reported path length over more than four orders of magnitude. Second, although individual tornadoes exhibit substantial variability, the highest event densities remain concentrated around a well-defined increasing trend. Finally, the conditional medians closely follow the global regression throughout most of the observable range, indicating that the relationship is not driven by a small number of extreme events.

The event-level regression yields an effective scaling exponent of $\alpha = 0.431$, with a 95% pairs-bootstrap confidence interval of $[0.427, 0.436]$.

This narrow confidence interval indicates that the exponent is well constrained by the available dataset despite the substantial event-to-event variability visible in the complete tornado population.

The slight difference between the two slopes reflects the different statistical nature of the estimators. Whereas the global regression incorporates the complete event distribution, including the progressive broadening of the conditional width distribution with increasing path length, the median estimator follows the central tendency within successive logarithmic bins. The close agreement between these independent estimates demonstrates that the observed width–length relationship is not an artefact of the fitting procedure.

The substantial scatter visible in Fig. 1 reflects the intrinsic diversity of tornado environments, storm modes, lifetimes, and observational uncertainties associated with damage-path surveys. Such variability is expected in a climatological catalogue spanning 75 years and nearly 70,000 events. Importantly, however, the bootstrap confidence intervals remain comparatively narrow over the well-sampled portion of the catalogue, indicating that the central geometric tendency is robustly constrained despite the broad event-to-event dispersion.

The measured exponent should therefore be interpreted as an effective population-level descriptor rather than as a deterministic law governing individual tornado evolution. Because the SPC catalogue combines tornadoes produced under a wide range of meteorological conditions and observational eras, the principal result of this analysis is the identification of a statistically robust geometric organization emerging at the population level rather than the existence of a universal scaling law for individual tornadoes.

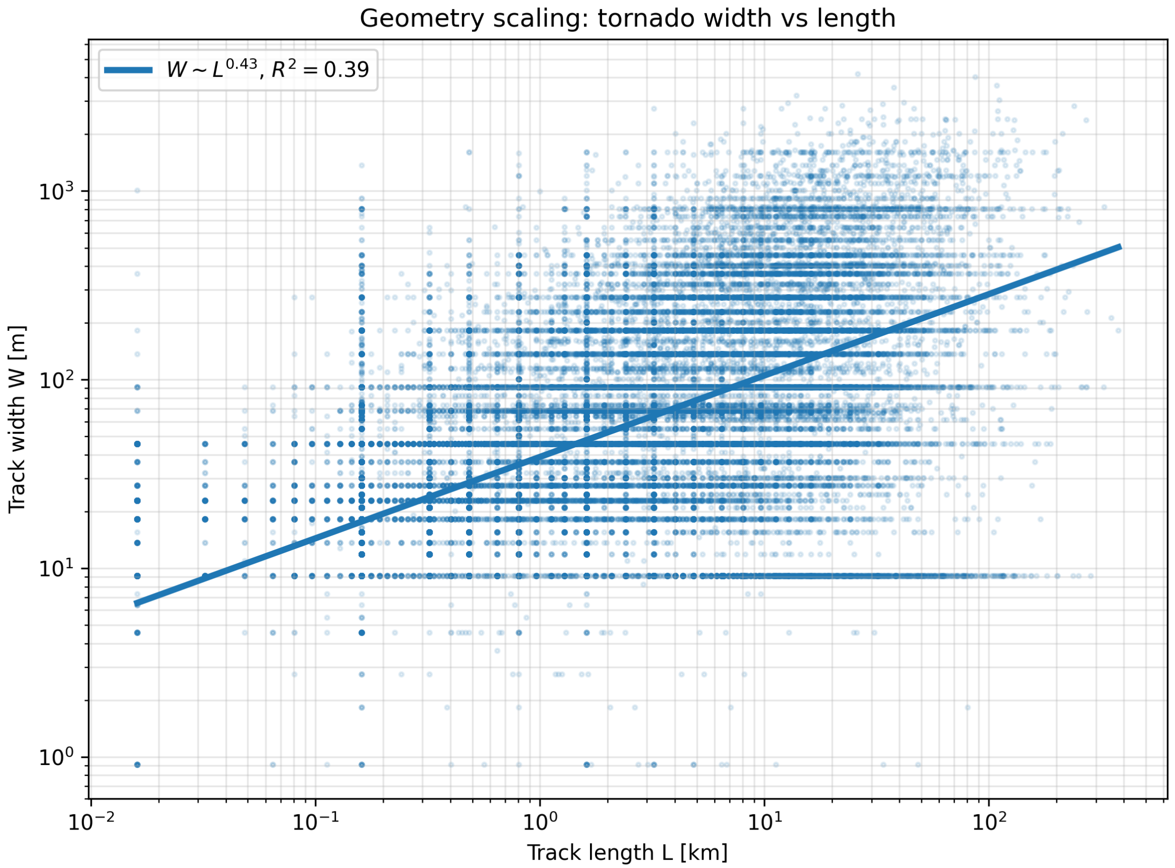


**Figure 1.** Relationship between reported tornado path length $L$ and reported maximum path width $W$ for the complete SPC tornado catalogue. Hexagonal colours represent logarithmic event density. The orange line denotes the global event-level regression, while the blue symbols show conditional median widths with 95% bootstrap confidence intervals. The event-level regression yields $\alpha = 0.431$ (95% pairs-bootstrap CI: 0.427–0.436).

### 3.2 Internal consistency of the geometric organization

The width–length relationship identified above naturally raises the question of whether the observed geometric organization remains self-consistent when derived observables are considered. To address this point, we examine the geometry-only quantity

$$A = LW,$$

which represents the simplest observable constructed exclusively from the reported path dimensions without introducing any intensity weighting.

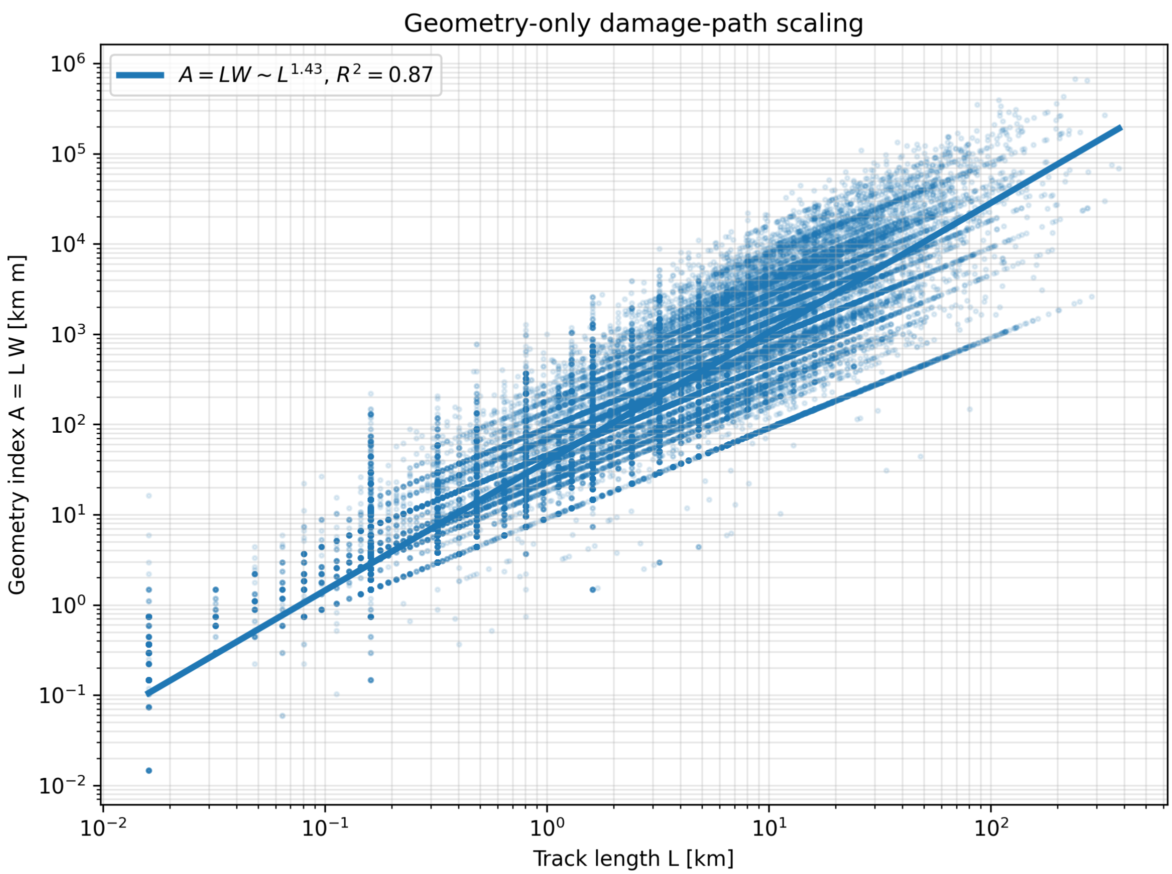


**Figure 2.** Scaling of the geometry-only observable $A = LW$ as a function of reported tornado path length $L$. The event-level regression, conditional medians, and their 95% bootstrap confidence intervals closely follow the scaling expected from the independently measured width–length relationship, providing an internal consistency check of the geometric organization.

Figure 2 shows that the derived observable follows a remarkably coherent scaling behaviour over the full observable range. The measured event-level exponent is nearly identical to that predicted from the independently estimated width–length relationship. Since

$$A = LW$$

and

$$W \sim L^{\alpha},$$

simple geometric consistency predicts

$$A \sim L^{1+\alpha},$$

which corresponds closely to the exponent obtained directly from the observations.

The significance of this result is therefore not the discovery of an additional scaling law, but the demonstration that the statistical organization identified in the previous subsection remains internally consistent when propagated to an independently derived geometric observable. In other words, the measured scaling of $A$ follows naturally from the correlated growth of reported path length and reported maximum path width rather than introducing a new independent relationship.

This consistency also demonstrates that the dominant organization is already present at the purely geometric level, before any EF-based intensity weighting is introduced. The geometry-only observable thus provides an important reference against which the intensity-weighted analyses presented later in the manuscript can be compared.

### 3.3 Robustness across observational periods and tornado populations

Having established the existence of a coherent population-level geometric organization, we next investigate whether this organization remains stable under two independent sources of variability: the substantial evolution of tornado reporting practices over the 1950–2024 period and the progressive restriction of the dataset to increasingly intense tornado populations.

We first consider temporal robustness. Figure 3 compares the complementary cumulative distribution functions (CCDFs) of the principal geometric observables.

The three observables display broad, strongly skewed distributions extending over several orders of magnitude. As expected, the smallest events are more sensitive to historical reporting practices, whereas the intermediate and upper parts of the distributions remain remarkably similar. These results suggest that the principal statistical organization is not restricted to a particular observational era.

To examine this point more directly, the catalogue is divided into the three independent historical periods introduced in Section 2.1. Figure 4 presents the distributions of the geometry-only observable before normalization.

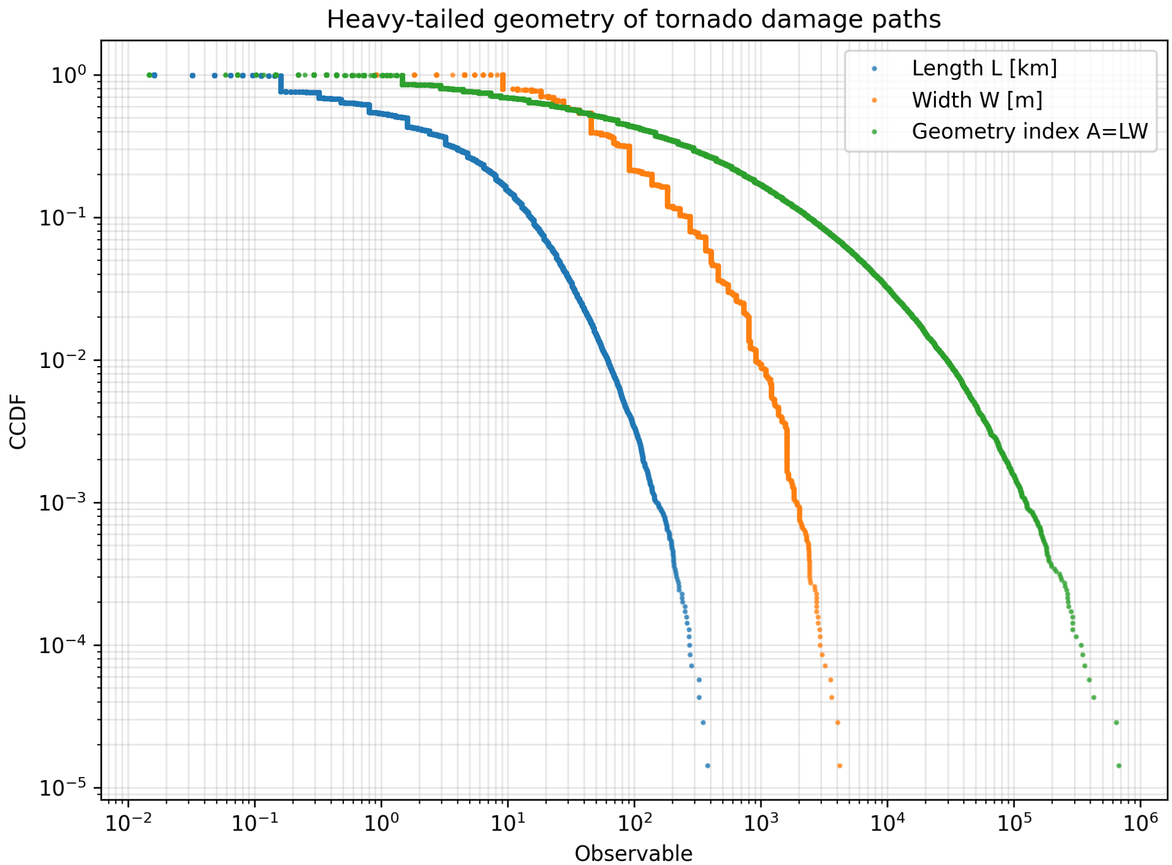


**Figure 3.** Complementary cumulative distribution functions of reported tornado path length $L$, reported maximum path width $W$, and the geometry-only observable $A = LW$. All three observables exhibit broad distributions extending over several orders of magnitude while preserving similar overall shapes throughout the SPC catalogue.

Moderate differences are visible, particularly for weak tornadoes during the earliest observational period, where reporting incompleteness is known to be greatest. Nevertheless, the overall distributional structures remain highly comparable.

Figure 5 presents the corresponding finite-size normalized distributions.

After normalization, a substantial overlap is obtained over the range containing the overwhelming majority of tornadoes. The remaining differences are confined primarily to the extreme tails, where sampling naturally becomes sparse. Rather than demonstrating strict universality, this comparison indicates that the dominant statistical organization is remarkably stable across successive observational eras.

Temporal robustness alone, however, does not exclude the possibility that the measured exponent simply reflects the predominance of weak tornadoes within the complete catalogue. We therefore repeated the analysis after progressively restricting the dataset to the EF0+, EF1+, EF2+, and EF3+ populations.

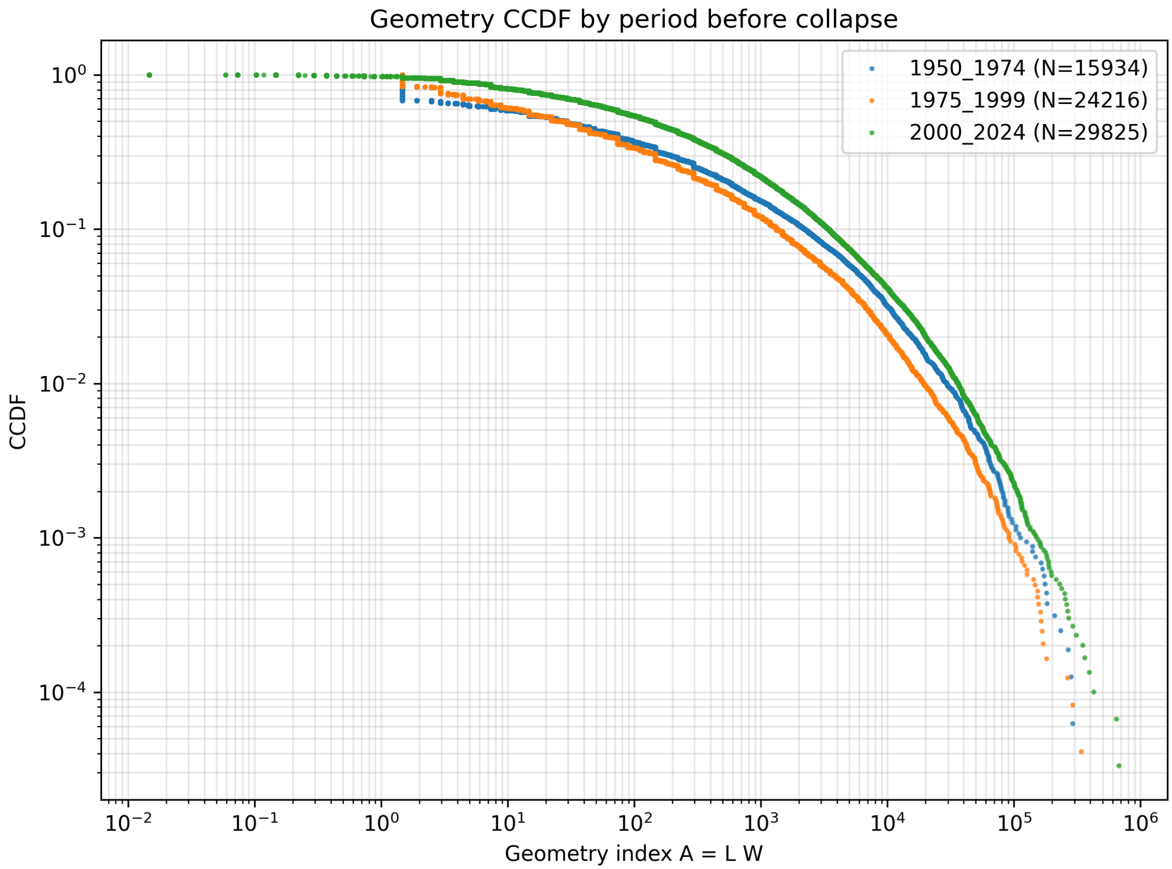


**Figure 4.** Distribution of the geometry-only observable $A = LW$ for the three historical periods before finite-size normalization. Differences are visible mainly for the smallest events, reflecting the evolution of tornado detection and reporting practices.

The effective exponent remains remarkably stable between the EF0+, EF1+, and EF2+ populations, with overlapping bootstrap confidence intervals. Only the EF3+ subset exhibits a noticeable increase in uncertainty, primarily because violent tornadoes represent only a small fraction of the SPC catalogue. Importantly, no systematic drift of the exponent with increasing intensity threshold is observed.

Taken together, the temporal analyses and the EF-threshold sensitivity tests provide two independent demonstrations of robustness. They show that the population-level geometric organization identified in the preceding sections is neither confined to a particular observational era nor dominated by a specific intensity class. Instead, it appears to represent a persistent statistical property of the climatological tornado population.

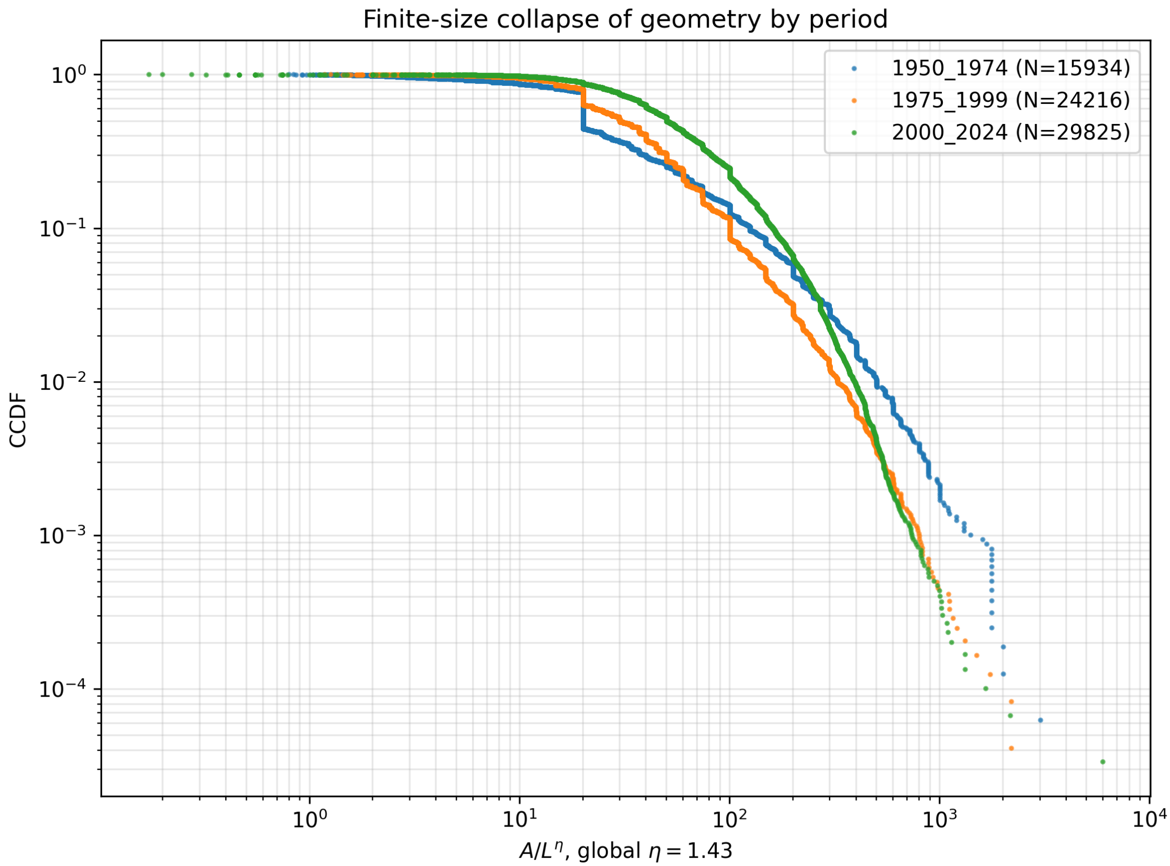


**Figure 5.** Finite-size normalized distributions of the geometry-only observable. After normalization, the three historical periods exhibit substantial overlap over the well-sampled portion of the catalogue, indicating that the dominant statistical organization remains stable despite major observational changes.

### 3.4 Propagation of the geometric organization to higher-order statistics

The previous sections established that tornado damage-path geometry is characterized by a robust population-level relationship linking reported path length and reported maximum path width. We now examine whether this organization remains consistent when higher-order statistical moments are considered.

For the geometry-only observable

$$A = LW,$$

the measured width–length relationship naturally implies that the conditional moments

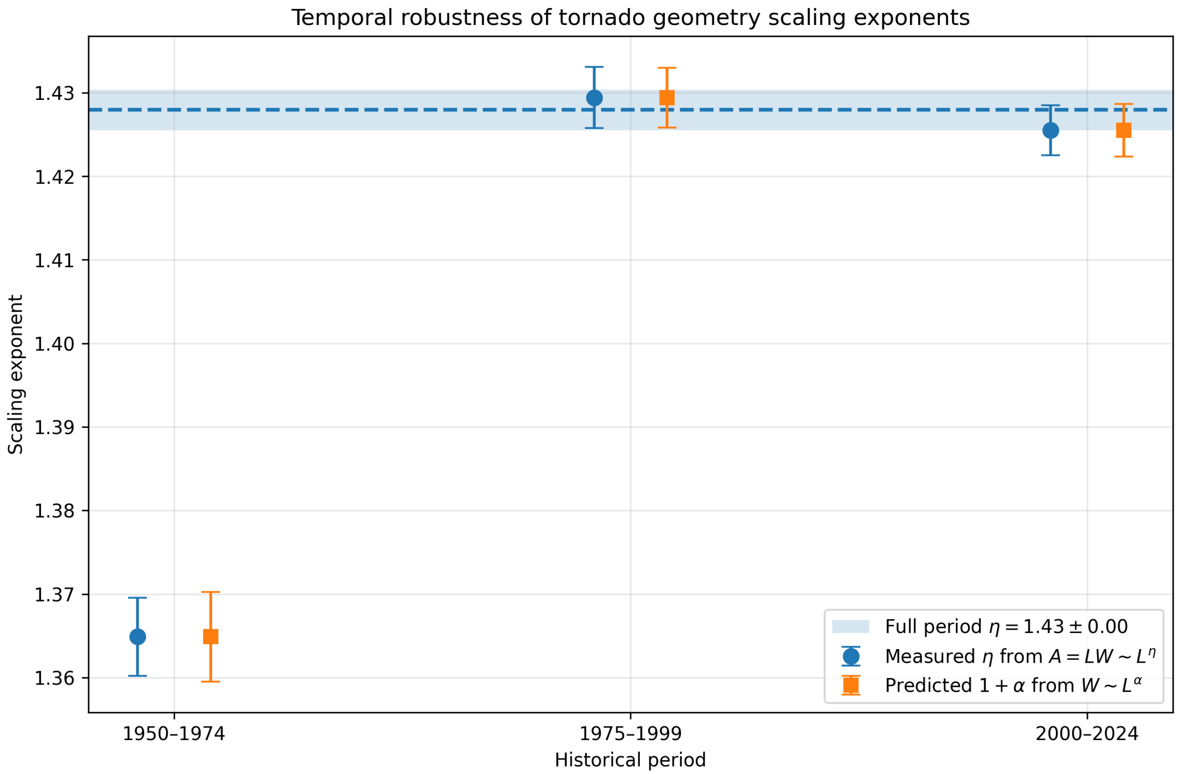


**Figure 6.** Robustness of the effective geometric scaling exponent for progressively stronger tornado populations. Error bars denote 95% bootstrap confidence intervals. The exponent remains statistically stable from the complete catalogue through the EF2+ subset, while the increased uncertainty for EF3+ reflects the much smaller number of available events.

$$M_q(L) = \langle A^q | L \rangle$$

should approximately satisfy an affine scaling relation over the range where the geometric organization remains statistically stable. The purpose of the present analysis is therefore not to identify an independent scaling law, but to evaluate the internal consistency of the geometric framework developed in the preceding sections.

We additionally compare the geometry-only observable with the geometry–intensity proxy

$$E \propto V^2 LW,$$

in order to assess whether the introduction of coarse EF-based intensity weighting substantially modifies the observed statistical organization.

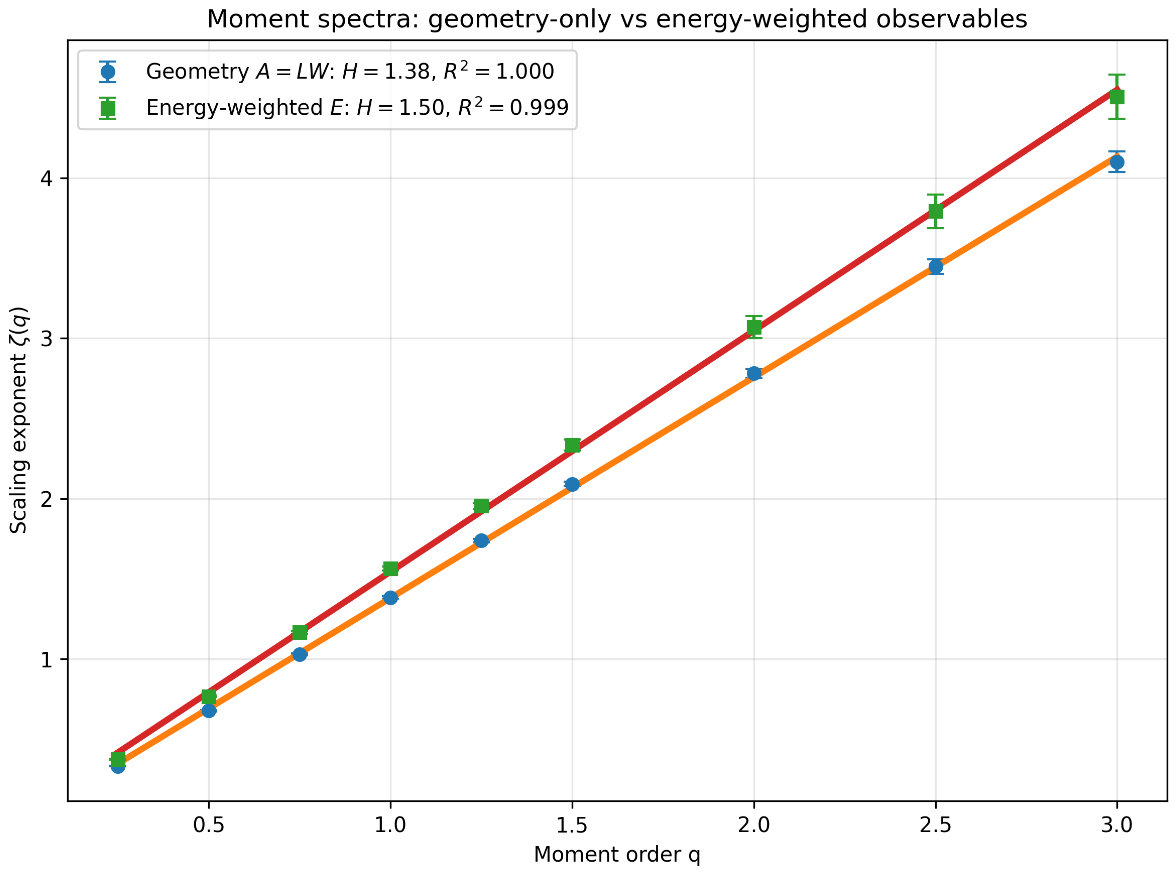


**Figure 7.** Scaling spectra of the conditional moments for the geometry-only observable $A = LW$ and the geometry–intensity proxy $E \propto V^2 LW$. Both observables exhibit predominantly affine behaviour over the well-resolved moment range, indicating that the principal statistical organization is already contained in the geometric observables.

Figure 7 shows that both observables exhibit predominantly affine scaling spectra over the interval

$$0.25 \le q \le 2,$$

which is well constrained by the available number of tornadoes. The geometry-only observable is accurately described by a single effective slope, while the geometry–intensity proxy exhibits a slightly steeper spectrum owing to the additional EF-based weighting. Nevertheless, the overall affine character remains essentially unchanged.

To evaluate possible departures from purely affine behaviour, the residuals relative to the best weighted linear fits are shown in Figure 8.

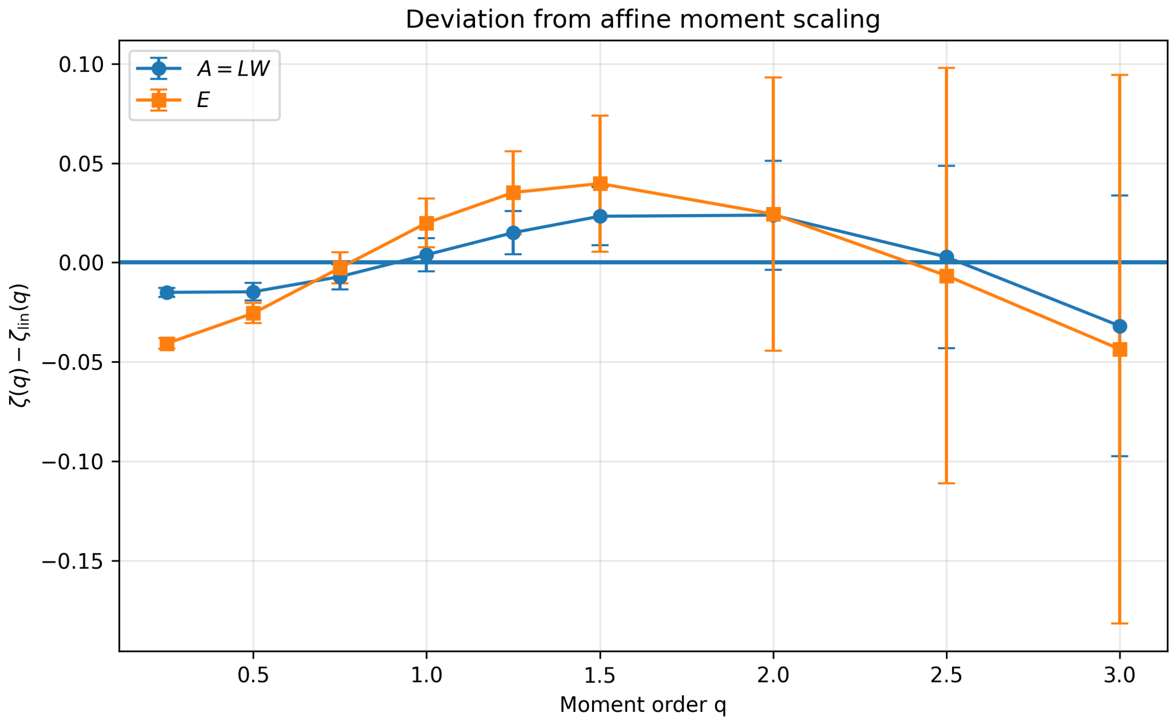


**Figure 8.** Residual deviations from the best affine approximation of the moment spectra. Weak departures from linearity become visible only for the highest investigated moments, where bootstrap uncertainties also increase substantially.

The residual analysis indicates that both spectra remain compatible with predominantly affine behaviour over the principal range of moments. Small departures from perfect linearity become visible only for moments above second order, where the statistics are increasingly controlled by the most extreme tornadoes and the associated bootstrap uncertainties grow rapidly. Consequently, the present dataset does not provide compelling evidence for robust multifractal corrections within the resolved moment range.

Taken together, these results demonstrate that the higher-order statistics remain fully consistent with the geometric organization identified from the first-order observables. The dominant statistical structure therefore originates primarily from the correlated evolution of reported path length and reported maximum path width, while the addition of coarse EF-based intensity information modifies only the overall scaling amplitude without altering the underlying organization.

### 3.5 Independent validation of the geometric organization

The analyses presented above consistently identify a robust population-level organization linking reported tornado path length and reported maximum path width. We finally examine two complementary tests designed to evaluate whether this organization could arise from trivial statistical effects or from the choice of a global regression model.

We first compare the observations with a series of null models in which the statistical dependence between reported path length and reported maximum path width is progressively removed while preserving the broad marginal distributions of the variables.

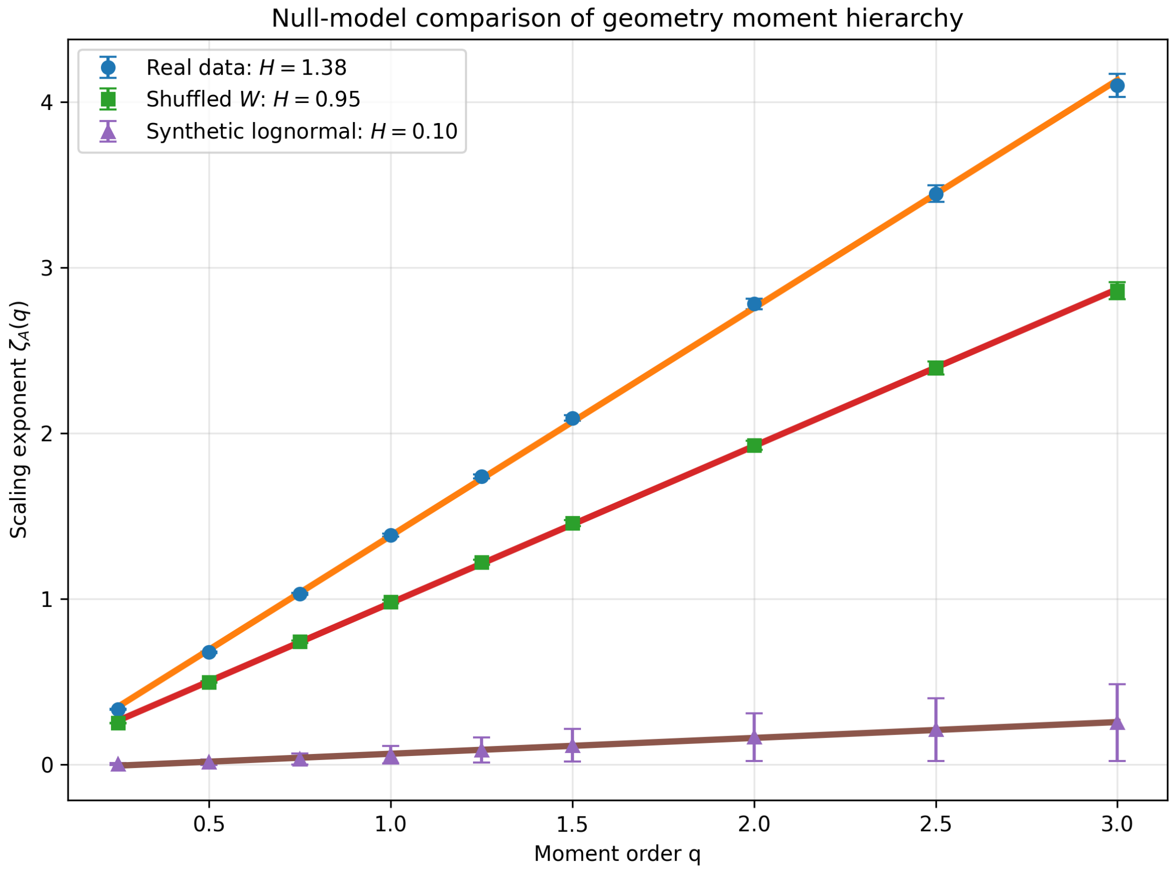


**Figure 9.** Comparison of the conditional-moment scaling spectra obtained from the observations, the shuffled-width model, and the synthetic lognormal population. Destroying the dependence between path length and width substantially weakens the observed hierarchy, demonstrating that the population-level organization cannot be explained solely by broad marginal distributions.

Removing the dependence between path length and width produces a marked reduction of the effective scaling exponent. Although the shuffled dataset preserves the empirical marginal distributions, it fails to reproduce the hierarchy observed in the SPC catalogue. The synthetic lognormal population departs even further from the observations, indicating that broad-tailed distributions alone are insufficient to generate the measured organization.

The same conclusion is obtained from the complementary cumulative distribution functions shown in Figure 10.

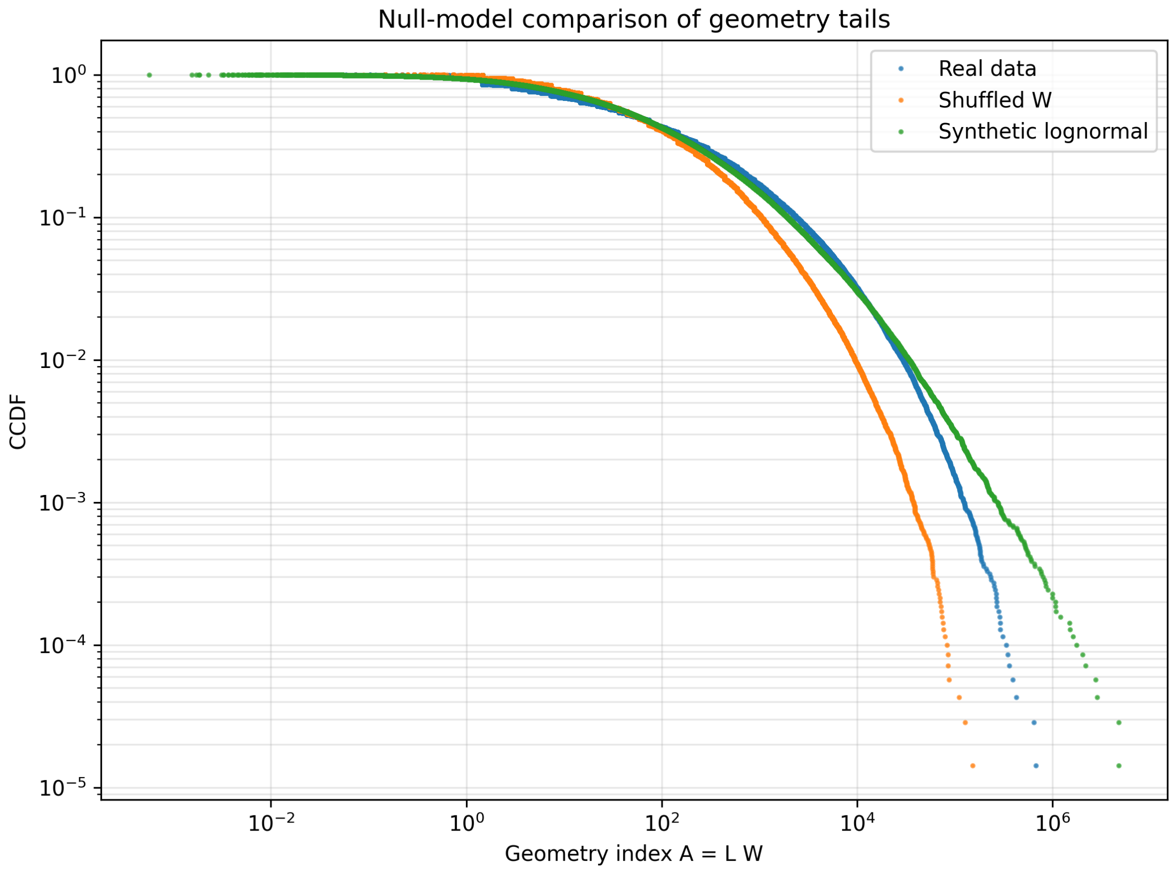


**Figure 10.** Complementary cumulative distribution functions for the observations and the corresponding null models. Although the synthetic populations reproduce broad-tailed distributions, they fail to reproduce the complete statistical organization observed in the real tornado population.

The null-model experiments therefore demonstrate that the observed hierarchy is not a trivial consequence of heavy-tailed marginal distributions or of the construction of the derived observables. Instead, it reflects genuine statistical dependence linking reported tornado path length and reported maximum path width.

A second validation is obtained from the local scaling analysis. Rather than estimating a single global exponent over the complete dataset, we compute the local logarithmic slope as a function of path length.

Following pronounced fluctuations at the smallest path lengths, the local exponent rapidly approaches a broad intermediate plateau that remains close to the global effective exponent over nearly two decades in scale. Larger fluctuations reappear only at the longest path lengths, where the number of available tornadoes decreases substantially and bootstrap uncertainties naturally increase.

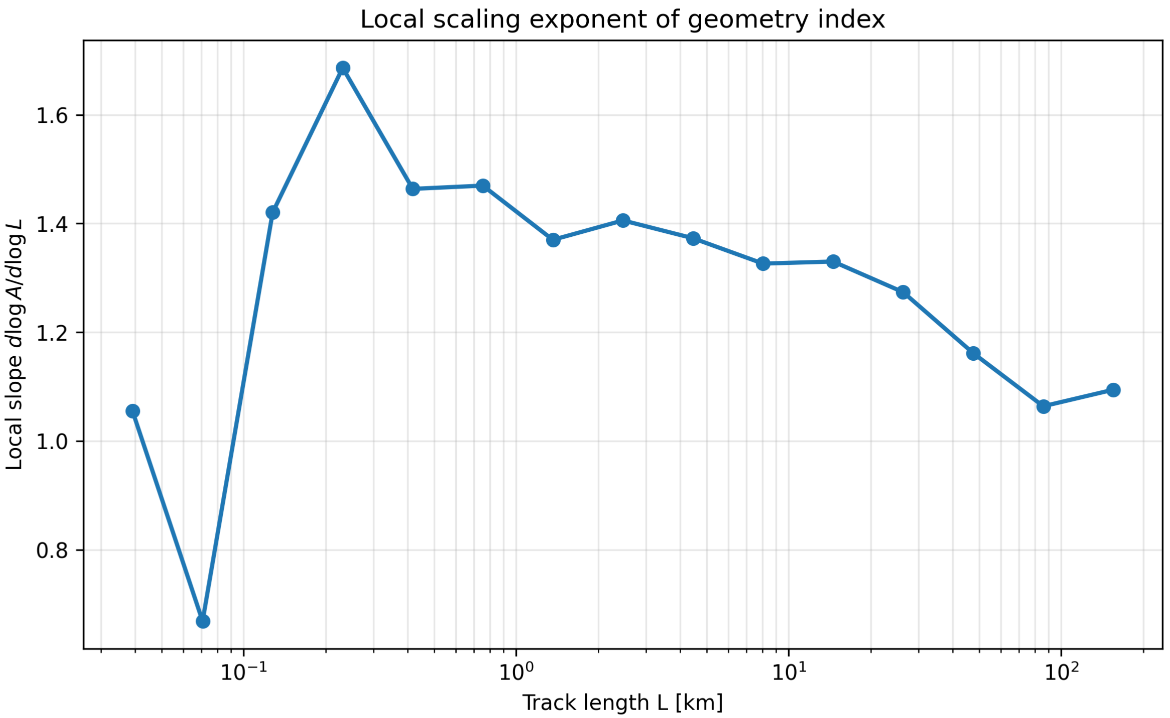


**Figure 11.** Local scaling exponent obtained using moving logarithmic windows. Over the well-sampled intermediate range, the local estimates remain broadly consistent with the global effective exponent, whereas the smallest and largest scales exhibit larger fluctuations owing to sampling limitations.

The broad intermediate region provides a complementary consistency check showing that the local estimates remain close to the global effective exponent over the best-sampled portion of the catalogue. Because no formal plateau boundary is imposed, this diagnostic is not used as stand-alone evidence for scale invariance and does not determine the principal conclusions of the study.

Taken together, the null-model experiments and the local scaling analysis provide two independent validations of the proposed geometric framework. The first demonstrates that the hierarchy requires genuine statistical dependence between path length and width, while the second shows that the observed organization persists locally across scales rather than emerging only from a global least-squares fit. These complementary analyses therefore reinforce the interpretation that the reported width–length relationship represents a robust population-level property of tornado climatology.

### 3.6 Summary of the statistical evidence

The analyses presented throughout this section provide a coherent and mutually consistent description of tornado damage-path geometry across the complete SPC catalogue.

Beginning with the direct relationship between reported tornado path length and reported maximum path width, we identified a robust population-level geometric organization that remains internally consistent when propagated to the derived geometry-only observable. This organization was shown to be stable across independent historical periods and progressively stronger tornado populations, indicating that it is neither an artefact of observational evolution nor a consequence of the predominance of weak tornadoes.

The higher-order statistical analyses further demonstrated that the conditional moment hierarchy is largely inherited from this underlying geometric organization. Both the geometry-only observable and the geometry–intensity proxy exhibit predominantly affine scaling spectra, while only weak departures from linearity appear at the highest moment orders, where sampling uncertainty naturally increases.

Finally, two independent validation strategies support the robustness of these conclusions. Null-model experiments show that broad marginal distributions alone cannot reproduce the observed organization once the dependence between reported path length and reported maximum path width is removed. Likewise, the local scaling estimates remain broadly consistent with the global effective exponent over the well-sampled portion of the catalogue, providing a complementary check that the measured organization is not produced solely by a single global regression.

Taken together, these results consistently support the existence of a robust population-level geometric organization within the SPC tornado catalogue. The physical interpretation of this statistical organization, its implications for tornado dynamics, and its limitations are discussed in the following section.

## 4 Discussion

The present study identifies a robust statistical organization linking reported tornado path length and reported maximum path width over the 69,975 tornadoes contained in the SPC database. Although individual tornadoes exhibit considerable variability in geometry, intensity, environment, and lifetime, the population as a whole displays a stable width–length relationship that persists across independent historical periods, tornado-intensity thresholds, and complementary statistical diagnostics. The convergence of these independent analyses—including event-level regression, conditional statistics, finite-size scaling, conditional moments, local scaling diagnostics, and null-model comparisons—provides consistent evidence that the observed geometric organization is not an artefact of a particular analysis technique.

It is important to emphasize that the geometry–intensity observable introduced in this work should not be interpreted as a direct estimate of tornado kinetic energy. Rather, it provides a simple phenomenological proxy that allows us to evaluate whether the statistical organization identified from geometry alone remains qualitatively unchanged after coarse EF-based intensity weighting. This interpretation is consistent with recent studies emphasizing both the difficulty of inferring tornado wind fields from damage observations (Miller et al., 2024) and the broader energetic perspective of atmospheric motion discussed by Tuck (2025).

An important consequence of this work is that the measured exponent should not be interpreted as a universal constant governing tornado dynamics. Instead, it represents an effective statistical descriptor of a heterogeneous climatological population combining different storm modes, environmental conditions, tornado intensities, and observational eras. The remarkable stability of this effective exponent nevertheless suggests that a coherent large-scale geometric organization emerges despite the substantial diversity of individual tornadoes.

This distinction is important for interpreting the scope of the present results. The analyses developed here do not establish a deterministic law capable of predicting the geometry of individual tornadoes. Instead, they demonstrate that robust statistical regularities emerge at the population level, providing a quantitative framework for describing the average organization of tornado damage paths. In this sense, the measured scaling relationship should be viewed as an empirical property of the climatological ensemble rather than as a dynamical law governing every individual event.

The consistency observed across the derived area observable, the conditional moment hierarchy, the temporal robustness analyses, and the null-model experiments further reinforces this interpretation. Rather than constituting independent scaling laws, these complementary diagnostics describe different statistical manifestations of the same underlying geometric organization. Taken together, they indicate that the principal result of the present study is not the identification of a single scaling exponent, but the emergence of a coherent population-level geometric structure that remains reproducible across multiple independent statistical perspectives.

The statistical organization identified in this study naturally raises the question of its physical origin. Although the present analysis is fundamentally climatological and does not directly resolve tornado dynamics, the measured width–length relationship is nevertheless compatible with several physical mechanisms governing the evolution of long-lived coherent vortices.

A first interpretation involves the coupled evolution of tornado translation, lifetime, and lateral growth. If the observed path length is viewed as the distance travelled by the tornado during its lifetime,

$$L \sim UT,$$

where $U$ denotes a characteristic translation velocity and $T$ the effective vortex lifetime, the measured scaling relationship implies that the transverse dimension of the damage path increases systematically, but sublinearly, as the tornado propagates. In this picture, longitudinal propagation and lateral broadening are not independent processes but reflect different aspects of the same evolving vortex.

Several physical mechanisms may contribute simultaneously to such behaviour. Progressive vortex stretching, turbulent entrainment, interaction with the near-surface boundary layer, environmental wind shear, and the evolving structure of the parent mesocyclone may all modify the lateral extent of the damaging wind field during the tornado lifetime. The observed statistical relationship therefore most likely represents the integrated signature of multiple interacting dynamical processes rather than the consequence of a single physical mechanism.

Interestingly, the measured exponent remains relatively close to the diffusive scaling

$$W \sim L^{1/2},$$

which characterizes a wide variety of stochastic growth processes. Although the measured value is statistically distinguishable from exactly one-half, this proximity suggests that lateral expansion may share some properties with constrained diffusive growth occurring under finite vortex coherence. Within this interpretation, longer-lived tornadoes do not simply travel farther while preserving a fixed transverse structure; instead, their damage paths broaden progressively as coherent vortex structures interact with their surrounding environment.

This interpretation remains intentionally qualitative. The present analysis does not identify the physical processes responsible for the measured exponent, nor does it demonstrate the existence of a unique self-similar growth mechanism. Rather, it identifies observational constraints that any future dynamical model of tornado evolution should be able to reproduce. In this sense, the measured geometric organization provides a statistical benchmark against which numerical simulations, reduced-order vortex models, and observational studies may be compared.

More broadly, the emergence of a stable geometric relationship despite the remarkable diversity of tornado environments suggests that common large-scale constraints may govern the evolution of tornado damage paths. Whether these constraints originate from vortex dynamics, parent-storm organization, environmental forcing, or a combination of these processes remains an open question that warrants further investigation.

The statistical interpretation of the measured scaling exponent also deserves careful discussion. Although the width–length relationship is remarkably stable across the complete SPC catalogue, it should not be interpreted as implying that individual tornadoes follow a unique deterministic geometric evolution. On the contrary, the broad dispersion observed throughout the dataset reflects the considerable diversity of tornado environments, parent-storm structures, lifetimes, and damage characteristics.

This distinction is illustrated by the conditional statistics developed in the present work. While the average geometric trend is robust, the conditional dispersion broadens progressively with path length, indicating that the statistical organization is intrinsically heteroscedastic. Tornadoes with longer reported paths exhibit a broader range of maximum path widths than shorter-track events, suggesting that the diversity of possible dynamical evolutions also increases with lifetime and propagation distance. Consequently, the measured exponent characterizes the evolution of the central tendency of the tornado population rather than a relationship with constant dispersion.

The hierarchy of conditional moments leads to the same conclusion. Over the range that is reliably resolved by the SPC catalogue, the scaling spectrum remains predominantly affine and is well described by a single effective exponent. Weak departures from perfect linearity become visible only when moments above second order are included. Because these higher-order moments are increasingly controlled by a very small fraction of the most extreme tornadoes, they are also associated with substantially larger statistical uncertainty. The present results therefore do not provide compelling evidence for robust multifractal corrections over the resolved range.

This interpretation is further supported by the null-model experiments. Broad marginal distributions alone are insufficient to reproduce the observed geometric organization once the statistical dependence between path length and path width is removed. Likewise, simple combinations of independent geometric variables and EF classifications fail to recover the ensemble of statistical diagnostics obtained from the observations. The organization identified here therefore reflects genuine statistical dependence between the reported path dimensions rather than a trivial consequence of heavy-tailed distributions.

Taken together, these results suggest that the effective exponent should be viewed as a population-level statistical descriptor emerging from the collective behaviour of a heterogeneous tornado ensemble. Its stability across independent observational periods, tornado-intensity thresholds, and complementary statistical diagnostics indicates that it captures a persistent large-scale property of tornado climatology, even though the physical mechanisms responsible for this organization almost certainly vary from one event to another.

The present study nevertheless has several important limitations that should be acknowledged.

First, the reported scaling relationships are inferred from tornado damage-path characteristics rather than from direct dynamical measurements of the vortices themselves. The SPC catalogue provides high-quality climatological information on tornado geometry but does not contain observations of the internal wind field, vortex circulation, pressure deficit, or turbulence intensity. Consequently, the statistical organization identified here should be interpreted as describing damage path morphology rather than the complete dynamics of tornado evolution.

Second, although the width–length relationship remains remarkably stable across historical periods and progressively stronger EF subsets, substantial observational heterogeneity inevitably remains within the catalogue. The database combines tornadoes produced by different storm modes, including supercells, quasi-linear convective systems, and landspouts, evolving under a broad range of environmental conditions. The effective scaling exponent reported here therefore represents an ensemble property of the complete climatological population rather than the characteristic behaviour of a single tornado class.

Third, the geometry–intensity observable considered in this study should not be interpreted as a direct estimate of tornado kinetic energy. Because EF ratings represent discrete damage-based intensity classes rather than continuous wind-speed measurements, the corresponding observable is necessarily a simplified geometry–intensity proxy. For this reason, the principal conclusions of the present work rely on the geometry-only observables, while the intensity-weighted analysis serves primarily as an independent consistency check.

These limitations naturally suggest several directions for future research. A first priority will be to investigate whether the effective width–length exponent remains stable within more homogeneous tornado populations separated according to storm mode, geographical region, or environmental conditions. Combining the present statistical framework with atmospheric reanalysis products such as ERA5 would make it possible to examine the influence of convective available potential energy (CAPE), vertical wind shear, storm-relative helicity (SRH), and parent-storm structure on the measured geometric organization.

An equally important extension concerns the connection between climatological scaling and explicit vortex dynamics. High-resolution Doppler-radar observations, numerical simulations, and reduced-order vortex models could be used to determine whether the effective population-level exponent identified here emerges naturally from the coupled evolution of vortex stretching, lateral growth, turbulent entrainment, and finite tornado lifetime. Such studies would help bridge the gap between the statistical organization documented in the present work and the physical mechanisms responsible for tornado evolution.

More generally, the present results illustrate how concepts originating from nonlinear dynamics and statistical physics can provide useful tools for characterizing severe-weather climatology. Rather than replacing process-based meteorological analyses, these approaches offer complementary constraints on the collective organization of tornado populations. The effective geometric relationships identified here may therefore serve as observational benchmarks for future theoretical, numerical, and observational studies seeking to explain the multiscale organization of tornado damage paths.

## 5 Conclusion

In this study, we investigated the statistical organization of tornado damage-path geometry using the NOAA Storm Prediction Center tornado database spanning the period 1950–2024. Rather than focusing on tornado occurrence frequencies or intensity statistics alone, we examined whether the reported path dimensions exhibit robust geometric organization across a large climatological population.

Our analyses reveal a stable statistical relationship linking reported tornado path length and reported maximum path width. This organization remains consistent across independent historical periods, progressively stronger tornado populations, and multiple complementary statistical diagnostics, including conditional statistics, finite-size scaling, conditional moments, local scaling analyses, and null-model comparisons. Together, these independent lines of evidence indicate that the observed geometric organization cannot be explained solely by broad marginal distributions or observational heterogeneity.

An important outcome of this work is that the measured scaling exponent should be interpreted as an effective statistical descriptor of the tornado population rather than as a universal dynamical constant. Despite the considerable diversity of tornado environments, storm modes, intensities, and lifetimes, the SPC catalogue exhibits a remarkably coherent population-level geometric organization. The associated hierarchy of conditional moments and the consistency of the derived geometric observables further suggest that this organization extends well beyond a simple pairwise correlation between path length and width.

Although the present analysis does not identify the physical mechanisms responsible for the observed organization, it establishes a robust set of observational constraints that future dynamical theories, numerical simulations, and high-resolution observational studies should be able to reproduce. In this sense, the statistical relationships reported here are better viewed as empirical benchmarks than as predictive laws governing individual tornadoes.

More broadly, the present work illustrates how concepts originating from statistical physics and nonlinear dynamics can complement traditional meteorological analyses by revealing emergent organization at the population level. The results suggest that tornado climatology contains a previously underexplored level of correlated geometric organization whose statistical structure remains stable despite the intrinsic intermittency, heterogeneity, and observational complexity of severe convective systems. The framework developed here is not restricted to tornado climatology and may prove useful for investigating the geometric organization of other intermittent geophysical hazards characterized by broad distributions, strong heterogeneity, and multiscale dynamics.

## Appendix A: Construction of geometric and intensity-weighted observables

### A1 Geometry-only observables

The primary objective of the present study is to investigate whether tornado damage-path geometry exhibits statistically robust organization independently of any intensity weighting. The analysis therefore begins with the two directly observed quantities provided by the NOAA Storm Prediction Center (SPC) database: the reported tornado path length, denoted by $L$, and the reported maximum path width, denoted by $W$.

From these variables, we define the geometry-only observable

$$A = LW, \tag{A1}$$

which serves as a simple descriptor of the overall geometrical extent of the reported damage path.

The quantity $A$ should not be interpreted as the exact physical damage area produced by a tornado. Actual damage depends on numerous factors, including land use, structural vulnerability, survey methodology, and the spatial continuity of damage. Instead, $A$ provides a coarse-grained geometric observable that allows the statistical organization of tornado morphology to be investigated without introducing additional free parameters.

More general combinations such as

$$L^a W^b$$

were deliberately not considered. Although additional exponents could be adjusted to improve empirical scaling relationships, doing so would introduce unnecessary degrees of freedom and complicate the physical interpretation. The observable defined by Eq. (A1) therefore represents the simplest geometry-only quantity naturally derived from the reported tornado dimensions.

### A2 Construction of the geometry–intensity observable

Although the principal analyses presented in this work rely exclusively on geometry-only observables, we additionally introduce a simple geometry–intensity quantity in order to examine whether the statistical organization identified from tornado geometry remains consistent after coarse intensity weighting.

The observable is defined as

$$E \propto V^2 LW, \tag{A2}$$

where $L$ denotes the reported tornado path length, $W$ the reported maximum path width, and $V$ a representative wind-speed amplitude associated with the corresponding EF category.

The construction of Eq. (A2) follows a simple dimensional argument. If the geometrical footprint of a tornado is represented by the geometry-only observable $A = LW$, then a first-order intensity weighting may be obtained by multiplying this quantity by the square of a characteristic wind speed. Constant factors, including air density, are absorbed into the proportionality constant because only relative scaling behaviour is investigated.

The introduction of Eq. (A2) is therefore motivated by comparative purposes rather than by the construction of a physically complete energy budget.

The quantity $E$ should not be interpreted as an estimate of the true kinetic energy of a tornado. The SPC database does not contain direct measurements of the vortex wind field, and the EF classification provides only discrete damage-based intensity categories. Consequently, Eq. (A2) defines a phenomenological geometry–intensity proxy rather than a physically resolved energetic observable.

For this reason, the principal conclusions of the present study are derived from the geometry-only observables. The analysis of Eq. (A2) is used only as an independent consistency check to determine whether the geometric organization remains qualitatively unchanged after coarse intensity weighting.

### A3 Representative EF-class wind speeds

The geometry–intensity observable introduced in Eq. (A2) requires a representative wind-speed amplitude for each Enhanced Fujita (EF) category. Following the operational NOAA wind-speed intervals, each EF class is assigned a single representative velocity corresponding to the midpoint of the associated velocity range.

The adopted values are summarized in Table A1.

**Table A1.** Representative wind-speed amplitudes assigned to the EF categories. Midpoint values are derived from the operational NOAA velocity intervals.

| EF class | Representative velocity ($\mathrm{m\,s^{-1}}$) |
|---|---|
| EF0 | 35.8 |
| EF1 | 49.2 |
| EF2 | 61.7 |
| EF3 | 74.8 |
| EF4 | 89.4 |
| EF5 | 100.6 |

The precise numerical values adopted for the representative wind speeds have only a limited influence on the statistical analyses presented in this work. Additional sensitivity tests performed using the lower and upper bounds of the NOAA velocity intervals produced only minor variations in the estimated scaling exponents. This behaviour indicates that the principal statistical organization is governed primarily by the correlated geometry of tornado damage paths rather than by the exact calibration of the EF-class velocity assignment. The observables defined in this appendix constitute the basis of all subsequent statistical analyses. The robustness of the associated scaling relationships with respect to sampling, bootstrap estimation, binning strategy, and null-model construction is examined in Appendix B.

## Appendix B: Robustness and uncertainty analyses

### B1 Bootstrap uncertainty estimation

Uncertainties associated with the principal scaling exponents were estimated using non-parametric bootstrap resampling. Event-level regressions were evaluated using pairs-bootstrap realizations, while conditional statistics were resampled independently within each logarithmic path-length bin.

Unless otherwise stated, all confidence intervals reported throughout the manuscript correspond to the 2.5th and 97.5th percentiles of 2,000 bootstrap realizations.

The bootstrap analysis was applied consistently to the global width–length relationship, the derived geometric observables, conditional moment spectra, and the EF-threshold sensitivity analyses. The resulting uncertainties remain small compared with the measured population-level scaling amplitudes, indicating that the principal statistical conclusions are well constrained by the size of the SPC catalogue.

### B2 Sensitivity to logarithmic binning

Several logarithmic discretizations were examined to evaluate the dependence of the statistical analyses on the choice of binning. The conditional statistics and moment hierarchies were recomputed using 10, 12, 15, and 20 logarithmic bins spanning the complete range of tornado path lengths.

The estimated scaling exponents exhibited only minor variations across these different discretizations, while the overall structure of the conditional moment hierarchy remained unchanged. The principal population-level organization identified in the present work is therefore not sensitive to the precise logarithmic partition adopted for the analysis.

### B3 Sensitivity to moment order

The conditional moment hierarchy was evaluated over a broad range of moment orders in order to assess the stability of the inferred scaling behaviour. The principal analysis presented in the main text focuses on the interval

$$0.25 \leq q \leq 2,$$

where the statistical estimates remain well constrained by the available number of tornadoes.

Higher-order moments,

$$2 < q \leq 3,$$

were also examined as exploratory sensitivity analyses. Because these moments are increasingly influenced by a small number of extreme events, their associated bootstrap uncertainties become progressively larger.

Across the principal interval, the measured scaling spectrum remains predominantly affine and is accurately described by a weighted linear representation. Although a weak departure from perfect linearity becomes visible when moments above second order are included, the magnitude of this curvature remains comparable to the bootstrap uncertainty. Consequently, the present dataset does not provide statistically compelling evidence for robust multifractal corrections over the resolved range of moments.

The principal conclusions of the present study therefore rely on the well-constrained low- and intermediate-order moments, while the higher-order analyses are interpreted primarily as qualitative consistency checks rather than as quantitative evidence for additional scaling regimes.

### B4 Null-model implementation

The null-model framework was designed to determine whether the observed statistical organization could arise solely from the marginal distributions of the geometric variables or whether it requires genuine statistical dependence between tornado path length and reported maximum path width.

Several reference datasets were considered throughout this study.

The first null model was obtained by randomly permuting the observed values of $W$ while preserving the empirical distribution of both $L$ and $W$. This procedure destroys the statistical dependence between the two variables while leaving their marginal distributions unchanged.

The second null model consists of independent synthetic lognormal distributions adjusted to reproduce approximately the first- and second-order moments of the observed path-length and path-width distributions. The lognormal distribution is employed only as a convenient broad-distribution reference model and is not intended to represent the complete statistics of atmospheric extremes.

Additional synthetic populations were generated by combining independent realizations of the geometric variables with randomly assigned EF categories. These experiments evaluate separately the influence of geometry and coarse intensity weighting on the derived statistical observables.

Each synthetic dataset was analysed using exactly the same computational pipeline as the SPC observations, including event-level regressions, conditional statistics, finite-size scaling, conditional moments, local scaling diagnostics, and bootstrap uncertainty estimation. Consequently, any differences between the observations and the null models originate from the statistical structure of the data rather than from differences in the analysis procedure.

None of the null models reproduced the complete ensemble of observational diagnostics simultaneously. In particular, removing the dependence between path length and path width systematically weakened the observed geometric organization, supporting the interpretation that the principal results reported in this study arise from genuine population-level statistical correlations rather than from broad marginal distributions alone.

## Appendix C: Additional statistical analyses

The statistical framework developed in the present study is not specific to tornado climatology. Similar combinations of broad distributions, effective scaling relationships, and population-level organization have been reported in several geophysical systems, including rainfall intermittency (Lovejoy and Schertzer, 1985; Tessier et al., 1993), earthquake statistics (Turcotte, 1997), wildfire occurrence (Malamud et al., 1998), and other nonequilibrium multiscale phenomena (Stanley et al., 1999; Sornette, 2006).

The comparison is intended only to highlight methodological similarities. The present analyses do not imply that tornadoes share identical dynamical mechanisms with these systems, nor do they establish the existence of universal scaling laws across geophysical hazards. Rather, they illustrate how statistical tools originating from nonlinear dynamics and statistical physics can provide complementary insight into the organization of heterogeneous climatological populations.

The methodology developed here may therefore be applied more generally to other geophysical hazards for which only population-level geometric descriptors are available, providing a common statistical framework for the comparative analysis of multiscale natural phenomena.

## References


Agee, E. and Childs, S.: Adjustments in Tornado Counts, F-Scale Intensity, and Path Width for Assessing Significant Tornado Destruction, Journal of Applied Meteorology and Climatology, 53, 1494–1505, https://doi.org/10.1175/JAMC-D-13-0235.1, 2014.

Bak, P., Tang, C., and Wiesenfeld, K.: Self-Organized Criticality: An Explanation of 1/f Noise, Physical Review Letters, 59, 381–384, https://doi.org/10.1103/PhysRevLett.59.381, 1987.

Brooks, H. E.: On the Relationship of Tornado Path Length and Width to Intensity, Weather and Forecasting, 19, 310–319, https://doi.org/10.1175/1520-0434(2004)019<0310:OTROTP>2.0.CO;2, 2004.

Corral, Á.: Long-Term Clustering, Scaling, and Universality in the Temporal Occurrence of Earthquakes, Physical Review Letters, 92, 108 501, https://doi.org/10.1103/PhysRevLett.92.108501, 2004.

Dutton, J. A.: The Ceaseless Wind: An Introduction to the Theory of Atmospheric Motion, Dover Publications, New York, 2 edn., ISBN 0486650960, 1986.

Edwards, R., LaDue, J. G., Ferree, J. T., Scharfenberg, K., Maier, C., and Coulbourne, W. L.: Changes in Tornado Climatology Accompanying the Enhanced Fujita Scale, Journal of Applied Meteorology and Climatology, 60, 1465–1482, https://doi.org/10.1175/JAMC-D-20-0263.1, 2021.

Elsner, J. B., Elsner, S. C., and Jagger, T. H.: Tornado Intensity Estimated from Damage Path Dimensions, PLOS ONE, 9, e107 571, https://doi.org/10.1371/journal.pone.0107571, 2014.

Gill, A. E.: Atmosphere–Ocean Dynamics, vol. 30 of *International Geophysics*, Academic Press, New York, ISBN 9780122835223, 1982.

Lovejoy, S. and Schertzer, D.: Generalized Scale Invariance in the Atmosphere and Fractal Models of Rain, Water Resources Research, 21, 1233–1250, https://doi.org/10.1029/WR021i008p01233, 1985.

Lovejoy, S. and Schertzer, D.: The Weather and Climate: Emergent Laws and Multifractal Cascades, Cambridge University Press, https://doi.org/10.1017/CBO9781139093801, 2013.

Malamud, B. D. and Turcotte, D. L.: Statistics of Severe Tornadoes and Severe Tornado Outbreaks, Atmospheric Chemistry and Physics, 12, 8459–8473, https://doi.org/10.5194/acp-12-8459-2012, 2012.

Malamud, B. D., Morein, G., and Turcotte, D. L.: Forest Fires: An Example of Self-Organized Critical Behavior, Science, 281, 1840–1842, https://doi.org/10.1126/science.281.5384.1840, 1998.

Miller, S. L., Kopp, G. A., Sills, D. M. L., and Butt, D. G.: Estimating Wind Speeds in Tornadoes Using Debris Trajectories of Large Compact Objects, Monthly Weather Review, 152, 1859–1881, https://doi.org/10.1175/MWR-D-23-0260.1, 2024.

Schertzer, D. and Lovejoy, S.: Physical Modeling and Analysis of Rain and Clouds by Anisotropic Scaling Multiplicative Processes, Journal of Geophysical Research, 92, 9693–9714, https://doi.org/10.1029/JD092iD08p09693, 1987.

Sornette, D.: Critical Phenomena in Natural Sciences: Chaos, Fractals, Selforganization and Disorder: Concepts and Tools, Springer, 2 edn., https://doi.org/10.1007/3-540-33182-4, 2006.

Stanley, H. E., Amaral, L. A. N., Buldyrev, S. V., Goldberger, A. L., Havlin, S., Ivanov, P. C., and Peng, C.-K.: Scaling and Universality in Animate and Inanimate Systems, Physica A, 270, 309–324, https://doi.org/10.1016/S0378-4371(99)00260-8, 1999.

Tessier, Y., Lovejoy, S., and Schertzer, D.: Universal Multifractals: Theory and Observations for Rain and Clouds, Journal of Applied Meteorology, 32, 223–250, https://doi.org/10.1175/1520-0450(1993)032<0223:UMTAOF>2.0.CO;2, 1993.

Tippett, M. K. and Cohen, J. E.: Tornado Outbreak Variability Follows Taylor's Power Law of Fluctuation Scaling and Increases Dramatically with Severity, Nature Communications, 7, 10 668, https://doi.org/10.1038/ncomms10668, 2016.

Tuck, A. F.: The Generation of Wind Velocity via Scale Invariant Gibbs Free Energy: Turbulence Drives the General Circulation, Entropy, 27, 740, https://doi.org/10.3390/e27070740, 2025.

Turcotte, D. L.: Fractals and Chaos in Geology and Geophysics, Cambridge University Press, 2 edn., https://doi.org/10.1017/CBO9781139174692, 1997.

Veneziano, D., Langousis, A., and Furcolo, P.: Multifractality and Rainfall Extremes: A Review, Water Resources Research, 42, W06D15, https://doi.org/10.1029/2005WR004716, 2006.